

A Brief Introduction to Wilson Loops and Large N

Yuri Makeenko

*Institute of Theoretical and Experimental Physics, Moscow, Russia**

A pedagogical introduction to Wilson loops, lattice gauge theory and the $1/N$ -expansion of QCD is presented. The three introductory lectures were given at the 37th ITEP Winter School of Physics, Moscow, February 9–16, 2009.

PACS numbers: 11.15.Pg, 11.15.Ha, 12.38.Aw

I. INTRODUCTION

In these lecture notes I give a brief pedagogical introduction to the methods used in nonperturbative investigations of QCD and other gauge theories. The main attention is paid to Wilson loops, both on the lattice and in the continuum, which play a central role in modern formulations of gauge theories and to the method of the $1/N$ expansion.

For further studies of this subject I can recommend the textbook [1] which contains detail references. In this text I restrict myself only with references to a few classical papers.

Lecture I Wilson loops

Wilson loops are essentially phase factors in Abelian or non-Abelian gauge theories. Wilson loops are observable in quantum theory by the Aharonov–Bohm effect. Wilson loops play a central role in the lattice formulation of gauge theories. QCD can be reformulated through the Wilson loops in a manifest gauge-invariant way. Analogues of the Wilson loops are extremely useful in solving various kinds of matrix models.

II. PHASE FACTORS IN QED

A. Definition and basic properties

Abelian phase factor is defined by the formula

$$U[\Gamma_{yx}] = e^{ie \int_{\Gamma_{yx}} dz^\mu A_\mu(z)}. \quad (1)$$

Under the gauge transformation

$$A_\mu(z) \xrightarrow{\text{g.t.}} A_\mu(z) + \frac{1}{e} \partial_\mu \alpha(z), \quad (2)$$

the Abelian phase factor transforms as

$$U[\Gamma_{yx}] \xrightarrow{\text{g.t.}} e^{i\alpha(y)} U[\Gamma_{yx}] e^{-i\alpha(x)}. \quad (3)$$

A wave function at the point x is transformed as

$$\varphi(x) \xrightarrow{\text{g.t.}} e^{i\alpha(x)} \varphi(x), \quad (4)$$

therefore the phase factor is transformed as the product $\varphi(y)\varphi^\dagger(x)$:

$$U[\Gamma_{yx}] \xrightarrow{\text{g.t.}} " \varphi(y) \varphi^\dagger(x) ". \quad (5)$$

A wave function at the point x transforms like one at the point y after multiplication by the phase factor:

$$U[\Gamma_{yx}] \varphi(x) \xrightarrow{\text{g.t.}} " \varphi(y) ", \quad (6)$$

and analogously

$$\varphi^\dagger(y) U[\Gamma_{yx}] \xrightarrow{\text{g.t.}} " \varphi^\dagger(x) ". \quad (7)$$

The phase factor plays the role of a parallel transporter in an electromagnetic field, and to compare phases of a wave function at points x and y , we should first make a parallel transport along some contour Γ_{yx} . The result is Γ -dependent except when $A_\mu(z)$ is a pure gauge (vanishing field strength $F_{\mu\nu}(z)$). Certain subtleties occur for not simply connected spaces (the Aharonov–Bohm effect).

B. Propagators in external field

Let us consider a quantum particle in a classical electromagnetic field. To introduce electromagnetic field, ∂_μ is to be replaced by the covariant derivative

$$\partial_\mu \longrightarrow \nabla_\mu = \partial_\mu - ieA_\mu(x). \quad (8)$$

For the propagator we get

$$G(x, y; A) = \frac{1}{2} \int_0^\infty d\tau e^{-\frac{1}{2}\tau m^2} \times \int_{\substack{z_\mu(0)=x_\mu \\ z_\mu(\tau)=y_\mu}} \mathcal{D}z_\mu(t) e^{-\frac{1}{2} \int_0^\tau dt \dot{z}_\mu^2(t) + ie \int_0^\tau dt z^\mu(t) A_\mu(z(t))}. \quad (9)$$

The exponent is just the classical (Euclidean) *action* of a particle in an external electromagnetic field. The path-integral representation (9) for the propagator of a scalar

*Electronic address: makeenko@itep.ru

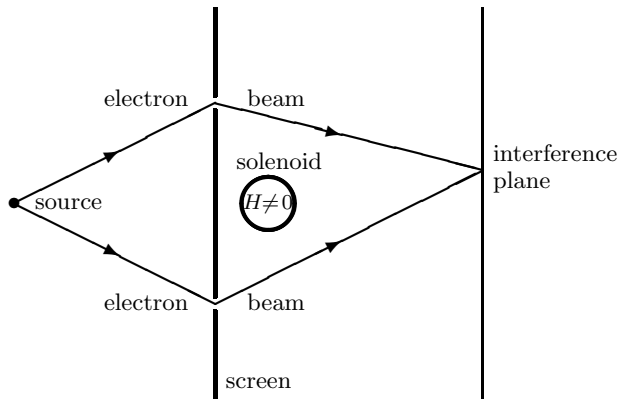


FIG. 1: Scheme of the Aharonov–Bohm experiment.

particle in an external electromagnetic field is due to Feynman.

We can alternatively rewrite Eq. (9) as

$$G(x, y; A) = \sum_{\Gamma_{yx}} e^{-S_{\text{free}}[\Gamma_{yx}] + ie \int_{\Gamma_{yx}} dz^\mu A_\mu(z)}, \quad (10)$$

where we represented the (parametric invariant) integral over dt as the contour integral along the trajectory Γ_{yx} over

$$dz^\mu = dt \dot{z}^\mu(t). \quad (11)$$

The transition amplitude of a quantum particle in a classical electromagnetic field is the sum over paths of the Abelian phase factor (1).

C. Aharonov–Bohm effect

Transverse components of the electromagnetic field describe photons. Longitudinal components are related to gauging the phase of a wave function, i.e. permit one to compare its values at different space-time points when an electron is placed in an external electromagnetic field.

In quantum mechanics, the wave-function phase itself is unobservable. Only the phase differences are observable, *e.g.* via interference phenomena. The phase difference depends on the value of the phase factor for a given path Γ_{yx} along which the parallel transport is performed.

The phase factors are observable in quantum theory, in contrast to classical theory. This is seen in the Aharonov–Bohm effect [2] whose scheme is depicted in Fig. 1. Electrons do not pass inside the solenoid where the magnetic field is concentrated. Nevertheless, a phase difference arises between the electron beams passing through the two slits. The interference picture changes with the value of the electric current.

The phase difference depends on (the real part of)

$$\begin{aligned} & e^{ie \int_{\Gamma_{yx}^+} dz^\mu A_\mu(z)} e^{-ie \int_{\Gamma_{yx}^-} dz^\mu A_\mu(z)} \\ &= e^{ie \oint_{\Gamma} dz^\mu A_\mu(z)} = e^{ie \int d\sigma^{\mu\nu} F_{\mu\nu}} = e^{ieHS}, \end{aligned} \quad (12)$$

where the closed contour Γ is composed from Γ_{yx}^+ and Γ_{yx}^- . It does not depend on the shape of Γ_{yx}^+ and Γ_{yx}^- but depends only on HS — the magnetic flux through the solenoid.

III. YANG-MILLS THEORIES

Modern theories of fundamental interactions are gauge theories. The principle of local gauge invariance was introduced by H. Weyl for the electromagnetic interaction in analogy with general covariance in Einstein’s theory of gravitation. An extension to non-Abelian gauge groups was given by Yang and Mills in 1954 [3].

A crucial role in gauge theories is played by the phase factor which is associated with parallel transport in an external gauge field. The phase factors are observable in quantum theory, in contrast to classical theory. This is analogous to the Aharonov–Bohm effect for the electromagnetic field.

A. Gauge invariance

The principle of local gauge invariance deals with the gauge transformation (g.t.) of a matter field ψ , which is given by

$$\psi(x) \xrightarrow{\text{g.t.}} \psi'(x) = \Omega(x) \psi(x). \quad (13)$$

Here $\Omega(x) \in G$ with G being a semisimple Lie group which is called the gauge group ($G = SU(3)$ for QCD). Equation (13) demonstrates that ψ belongs to the fundamental representation of G .

The unitary gauge group is when

$$\Omega^{-1}(x) = \Omega^\dagger(x), \quad (14)$$

while an extension to other Lie groups is straightforward. Then we have

$$\psi^\dagger(x) \xrightarrow{\text{g.t.}} \psi'^\dagger(x) = \psi^\dagger(x) \Omega^\dagger(x). \quad (15)$$

In analogy with QCD, the gauge group $G = SU(N)$ is usually associated with color and the proper index of ψ is called the color index.

The gauge transformation (13) of the matter field ψ can be compensated by a transformation of the non-Abelian gauge field \mathcal{A}_μ which belongs to the adjoint representation of G :

$$\begin{aligned} & \mathcal{A}_\mu(x) \xrightarrow{\text{g.t.}} \mathcal{A}'_\mu(x) \\ &= \Omega(x) \mathcal{A}_\mu(x) \Omega^\dagger(x) + i \Omega(x) \partial_\mu \Omega^\dagger(x). \end{aligned} \quad (16)$$

It is convenient to introduce the Hermitian matrix

$$[\mathcal{A}_\mu(x)]^{ij} = g \sum_a A_\mu^a(x) [t^a]^{ij}, \quad (17)$$

where g is the gauge coupling constant.

The matrices $[t^a]^{ij}$ are the generators of G ($a = 1, \dots, N^2 - 1$ for $SU(N)$) which are normalized such that

$$\text{tr } t^a t^b = \delta^{ab}, \quad (18)$$

where tr is the trace over the matrix indices i and j .

Quite often another normalization of the generators with an extra factor of $1/2$, $\text{tr } \tilde{t}^a \tilde{t}^b = \frac{1}{2} \delta^{ab}$, is used for historical reasons, in particular $\tilde{t}^a = \sigma^a/2$ for the $SU(2)$ group, where σ^a are the Pauli matrices. This results in the redefinition of the coupling constant, $\tilde{g}^2 = 2g^2$.

Equation (17) can be inverted to give

$$A_\mu^a(x) = \frac{1}{g} \text{tr } \mathcal{A}_\mu(x) t^a. \quad (19)$$

Substituting

$$\Omega(x) = e^{i\alpha(x)}, \quad (20)$$

we obtain for an infinitesimal α :

$$\delta \mathcal{A}_\mu(x) \stackrel{\text{g.t.}}{=} \nabla_\mu^{\text{adj}} \alpha(x). \quad (21)$$

Here

$$\nabla_\mu^{\text{adj}} \alpha \equiv \partial_\mu \alpha - \imath [\mathcal{A}_\mu, \alpha] \quad (22)$$

is the covariant derivative in the adjoint representation of G , while

$$\nabla_\mu^{\text{fun}} \psi \equiv \partial_\mu \psi - \imath \mathcal{A}_\mu \psi \quad (23)$$

is that in the fundamental representation. It is evident that

$$\nabla_\mu^{\text{adj}} B(x) = [\nabla_\mu^{\text{fun}}, B(x)], \quad (24)$$

where $B(x)$ is a matrix-valued function of x .

The QCD action is given in the matrix notation as

$$\begin{aligned} S[\mathcal{A}, \psi, \bar{\psi}] \\ = \int d^4x \left[\bar{\psi} \gamma_\mu (\partial_\mu - \imath \mathcal{A}_\mu) \psi + m \bar{\psi} \psi + \frac{1}{4g^2} \text{tr } \mathcal{F}_{\mu\nu}^2 \right], \end{aligned} \quad (25)$$

where

$$\mathcal{F}_{\mu\nu} = \partial_\mu \mathcal{A}_\nu - \partial_\nu \mathcal{A}_\mu - \imath [\mathcal{A}_\mu, \mathcal{A}_\nu] \quad (26)$$

is the (Hermitian) matrix of the non-Abelian field strength.

This action is invariant under the local gauge transformation since

$$\mathcal{F}_{\mu\nu}(x) \stackrel{\text{g.t.}}{\longrightarrow} \Omega(x) \mathcal{F}_{\mu\nu}(x) \Omega^\dagger(x) \quad (27)$$

or

$$\delta \mathcal{F}_{\mu\nu}(x) \stackrel{\text{g.t.}}{=} -\imath [\mathcal{F}_{\mu\nu}(x), \alpha(x)] \quad (28)$$

for the infinitesimal gauge transformation.

For the Abelian group $G = U(1)$, the formulas recover those for QED.

B. Non-Abelian phase factors (Wilson loops)

To compare phases of wave functions at distinct points, a non-Abelian extension of the parallel transporter is needed. The proper extension of the Abelian formula (1):

$$U[\Gamma_{yx}] = P e^{\imath \int_{\Gamma_{yx}} dz^\mu \mathcal{A}_\mu(z)}, \quad (29)$$

includes the symbol P of path-ordering.

Although the matrices $\mathcal{A}_\mu(z)$ do not commute, the path-ordered exponential on the RHS of Eq. (29) is defined unambiguously. This is obvious after rewriting the phase factor in an equivalent form

$$P e^{\imath \int_{\Gamma_{yx}} dz^\mu \mathcal{A}_\mu(z)} = P e^{\imath \int_0^\tau dt \dot{z}^\mu(t) \mathcal{A}_\mu(z(t))}. \quad (30)$$

The path-ordered exponential in Eq. (29) can be understood as

$$U[\Gamma_{yx}] = \prod_{t=0}^\tau [1 + \imath dt \dot{z}^\mu(t) \mathcal{A}_\mu(z(t))]. \quad (31)$$

Using Eq. (11), Eq. (31) can also be written as

$$U[\Gamma_{yx}] = \prod_{z \in \Gamma_{yx}} [1 + \imath dz^\mu \mathcal{A}_\mu(z)]. \quad (32)$$

If the contour Γ_{yx} is discretized, then the non-Abelian phase factor is approximated by

$$\begin{aligned} U[\Gamma_{yx}] \\ = \lim_{M \rightarrow \infty} \prod_{i=1}^M \left[1 + \imath (z_i - z_{i-1})^\mu \mathcal{A}_\mu \left(\frac{z_i + z_{i-1}}{2} \right) \right], \end{aligned} \quad (33)$$

which obviously reproduces (32) in the limit $z_{i-1} \rightarrow z_i$.

The non-Abelian phase factor (29) is an element of the gauge group G itself, while \mathcal{A}_μ belongs to the Lie algebra of G .

Matrices are rearranged in inverse order under Hermitian conjugation:

$$U^\dagger[\Gamma_{yx}] = U[\Gamma_{xy}]. \quad (34)$$

The notation Γ_{yx} means the orientation of the contour from x to y , while Γ_{xy} denotes the opposite orientation from y to x . These two result in opposite orders of multiplication for the matrices in the path-ordered product.

The phase factors obey the backtracking (*zig-zag*) condition

$$U[\Gamma_{yx}] U[\Gamma_{xy}] = 1. \quad (35)$$

The gauge field \mathcal{A}_μ in the discretized phase factor (33) is chosen at the *center* of the i th interval in order to satisfy Eq. (35) at finite discretization.

Under the gauge transformation (16) $U[\Gamma_{yx}]$ transforms as

$$U[\Gamma_{yx}] \stackrel{\text{g.t.}}{\longrightarrow} \Omega(y) U[\Gamma_{yx}] \Omega^\dagger(x). \quad (36)$$

This formula stems from the fact that

$$\begin{aligned} [1 + \mathbb{1} dz^\mu \mathcal{A}_\mu(z)] &\xrightarrow{\text{g.t.}} [1 + \mathbb{1} dz^\mu \mathcal{A}'_\mu(z)] \\ &= \Omega(z + dz) [1 + \mathbb{1} dz^\mu \mathcal{A}_\mu(z)] \Omega^\dagger(z) \end{aligned} \quad (37)$$

which can be proven by substituting Eq. (16), so that $\Omega^\dagger(z)$ and $\Omega(z)$ *cancel* in the definition (32) at the intermediate point z .

A consequence of Eq. (36) is that $\psi(x)$, transported by the matrix $U[\Gamma_{yx}]$ to the point y , transforms under the gauge transformation as $\psi(y)$:

$$U[\Gamma_{yx}] \psi(x) \xrightarrow{\text{g.t.}} \psi(y). \quad (38)$$

Therefore, $U[\Gamma_{yx}]$ is, indeed, a parallel transporter.

It follows from these formulas that $\bar{\psi}(y) U[\Gamma_{yx}] \psi(x)$ is gauge invariant:

$$\bar{\psi}(y) U[\Gamma_{yx}] \psi(x) \xrightarrow{\text{g.t.}} \bar{\psi}(y) U[\Gamma_{yx}] \psi(x). \quad (39)$$

Another consequence of Eq. (36) is that the trace of the phase factor for a closed contour Γ is gauge invariant:

$$\text{tr} P e^{\mathbb{1} \oint_\Gamma dz^\mu \mathcal{A}_\mu(z)} \xrightarrow{\text{g.t.}} \text{tr} P e^{\mathbb{1} \oint_\Gamma dz^\mu \mathcal{A}_\mu(z)}. \quad (40)$$

This is quite similar to the Abelian phase factor.

The sufficient and necessary condition for the phase factor to be independent on a local variation of the path is the *vanishing* of $\mathcal{F}_{\mu\nu}$. The formulas of this type are well-known in differential geometry where parallel transport around a small closed contour determines the curvature. $\mathcal{F}_{\mu\nu}$ in Yang–Mills theory is the proper curvature in an internal color space while \mathcal{A}_μ is the connection.

A historical remark

An analog of the phase factor was first introduced by H. Weyl in 1919 [4] in his attempt to describe gravitational and electromagnetic interactions of electron on equal footing. What he did is associated in modern language with the scale rather than the gauge transformation, i.e. the vector-potential was not multiplied by $\mathbb{1}$ as in Eq. (1). This explains the term “gauge invariance” – gauging literally means fixing a scale.

The factor of $\mathbb{1}$ was inserted by London in 1927 [5] after creation of quantum mechanics and the recognition that the electromagnetic interaction corresponds to the freedom of choice of the phase of a wave function and not to a scale transformation.

Lecture II

Lattice gauge theories

Lattice gauge theories were proposed by Wilson in 1974 [6] to explain quark confinement in QCD. Lattice

gauge theory is a nonperturbative regularization of gauge theory and its nontrivial definition beyond perturbation theory. It provides a nonperturbative quantization of gauge fields by a lattice. Lattice gauge theories uses an analogy between quantum field theory and statistical mechanics and offers a possibility of applying nonperturbative methods: the strong-coupling expansion or the numerical Monte Carlo method to QCD, which provide evidence for quark confinement.

IV. LATTICE FORMULATION

A. The lattice

A lattice approximates continuous space by a discrete set of points. In Euclidean formulation the lattice is along all four coordinates, while the time is left continuous in Hamiltonian approach.

The lattice is defined as a set of points of d -dimensional Euclidean space with coordinates

$$x_\mu = n_\mu a, \quad (41)$$

where the components of the vector

$$n_\mu = (n_1, n_2, \dots, n_d) \quad (42)$$

are integer numbers. The points (41) are called the lattice sites.

The dimensional constant a , which equals the distance between the neighboring sites, is called the lattice spacing. Dimensional quantities are measured in units of a , thereby setting $a = 1$.

A 2d lattice with periodic boundary conditions is depicted in Fig. 2. Sites with the same numbers are identified. The spatial size of the lattice has $L_1 = 6$ and $L_2 = 4$. An analogous 4d lattice is called hypercubic.

The next concepts are the link and plaquette of a lattice which are shown in Fig. 3. A link $l = \{x; \mu\}$ connects two neighboring sites x and $x + a\hat{\mu}$, where $\hat{\mu}$ is a unit vector along the μ -direction ($\mu = 1, \dots, d$). A plaquette $p = \{x; \mu, \nu\}$ is the elementary square enclosed by

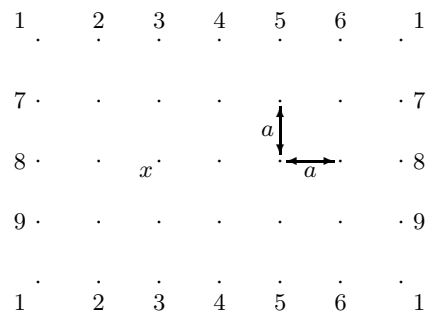


FIG. 2: Two-dimensional lattice with periodic boundary conditions.

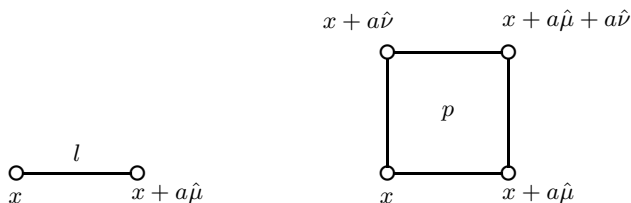


FIG. 3: Link (left) and plaquette (right).

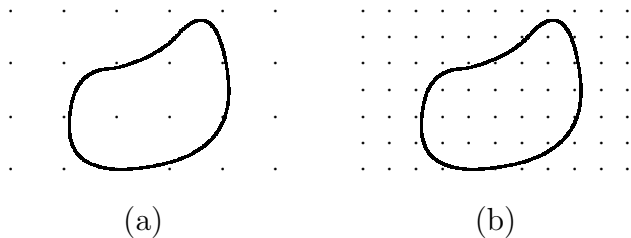


FIG. 4: Description of continuum configurations by lattices.

four links in the directions μ and ν . The set of four links which bound the plaquette p is denoted as ∂p .

For an infinite lattice, the number of degrees of freedom = ∞ (but enumerable). To limit the this number, the lattice has a finite size $L_1 \times L_2 \times \dots \times L_d$ in all directions. Periodic boundary conditions are usually imposed to reduce finite-size effects.

B. Matter and gauge fields on the lattice

Matter field, say a quark field, is attributed to the *lattice sites*, therefore a continuous field $\varphi(x)$ is approximated by its values at the lattice sites

$$\varphi(x) \implies \varphi_x. \quad (43)$$

The lattice field φ_x is a good approximation of a continuous field $\varphi(x)$ when $a \ll$ than the characteristic size of a given configuration. A description of continuum field configuration by lattices is illustrated by Fig. 4. Lattice (a) is “coarse” and can represent the given continuum field configuration very roughly, while lattice (b) is “fine” and its spacing is small enough.

The gauge field is attributed to the *links* of the lattice:

$$\mathcal{A}_\mu(x) \implies U_\mu(x). \quad (44)$$

It looks natural since a link is characterized by a coordinate and a direction – the same as $\mathcal{A}_\mu(x)$. Sometimes the notation $U_{x,\mu}$ is used as an alternative for $U_\mu(x)$ to emphasize that it is attributed to links.

The link variable $U_\mu(x)$ can be viewed as

$$U_\mu(x) = P e^{i \int_x^{x+a\hat{\mu}} dz^\mu \mathcal{A}_\mu(z)}, \quad (45)$$

where the integral is along the link $\{x; \mu\}$. As $a \rightarrow 0$, this yields

$$U_\mu(x) \rightarrow e^{ia\mathcal{A}_\mu(x)} \quad (46)$$

so that $U_\mu(x)$ is expressed via the exponential of the μ th component of the vector potential at the center of the link.

Since the path-ordered integral in Eq. (45) depends on the orientation, links are oriented. The same link, which connects the points x and $x+a\hat{\mu}$, can be written either as $\{x; \mu\}$ or as $\{x+a\hat{\mu}; -\mu\}$. The orientation is positive for $\mu > 0$ in the former case (i.e. the same as the direction of the coordinate axis) and is negative in the latter case.

The link variable $U_\mu(x)$ is assigned to links with positive orientations. The U -matrices which are assigned to links with negative orientations are given by

$$U_{-\mu}(x+a\hat{\mu}) = U_\mu^\dagger(x). \quad (47)$$

This is a one-link analog of Eq. (34).

It is clear from the relation (45) between the lattice and continuum gauge variables how to construct lattice phase factors (Wilson loops) – to construct the contours from the links of the lattice.

C. The Wilson action

An important role in the lattice formulation is played by the phase factor for the simplest closed contour on the lattice: the (oriented) boundary of a plaquette. The plaquette variable is composed from the link variables (45) as

$$U(\partial p) = U_\nu^\dagger(x) U_\mu^\dagger(x+a\hat{\nu}) U_\nu(x+a\hat{\mu}) U_\mu(x). \quad (48)$$

The link variable transforms under the gauge transformation as

$$U_\mu(x) \xrightarrow{\text{g.t.}} \Omega(x+a\hat{\mu}) U_\mu(x) \Omega^\dagger(x), \quad (49)$$

where the matrix $\Omega(x)$ is attributed to the lattice sites. This defines the lattice gauge transformation.

The plaquette variable transforms under the lattice gauge transformation as

$$U(\partial p) \xrightarrow{\text{g.t.}} \Omega(x) U(\partial p) \Omega^\dagger(x). \quad (50)$$

Its trace over the color indices is gauge invariant:

$$\text{tr} U(\partial p) \xrightarrow{\text{g.t.}} \text{tr} U(\partial p). \quad (51)$$

This invariance is used in constructing an action of a lattice gauge theory. The simplest Wilson action is

$$S_{\text{lat}}[U] = \sum_p \left[1 - \frac{1}{N} \text{Re tr} U(\partial p) \right]. \quad (52)$$

The summation is over all the elementary plaquettes of the lattice (i.e. over all x , μ , and ν), regardless of their orientations.

Since a reversal of the orientation results in complex conjugation:

$$\text{tr } U(\partial p) \xrightarrow{\text{reor.}} \text{tr } U^\dagger(\partial p) = [\text{tr } U(\partial p)]^*, \quad (53)$$

the action can be rewritten as the sum over oriented plaquettes

$$S_{\text{lat}}[U] = \frac{1}{2} \sum_{\text{orient } p} \left[1 - \frac{1}{N} \text{tr } U(\partial p) \right]. \quad (54)$$

As $a \rightarrow 0$, the lattice action (52) becomes the action of continuum gauge theory. To show this, we note that

$$U(\partial p) \rightarrow \exp [ia^2 \mathcal{F}_{\mu\nu}(x) + \mathcal{O}(a^3)], \quad (55)$$

where $\mathcal{F}_{\mu\nu}(x)$ is non-Abelian field strength (26).

In the Abelian theory, the expansion (55) is easily found from the Stokes theorem. The commutator of $\mathcal{A}_\mu(x)$ and $\mathcal{A}_\nu(x)$, which arises in the non-Abelian case, complements the field strength to the non-Abelian one, as is ensured by the gauge invariance.

A transition to the continuum limit is performed as

$$a^4 \sum_p \dots \xrightarrow{a \rightarrow 0} \frac{1}{2} \int d^4x \sum_{\mu,\nu} \dots \quad (56)$$

Expanding the RHS of Eq. (55) in a , we reproduce the continuum action

$$S_{\text{lat}} \xrightarrow{a \rightarrow 0} \frac{1}{4N} \int d^4x \sum_{\mu,\nu} \text{tr } \mathcal{F}_{\mu\nu}^2(x). \quad (57)$$

D. The Haar measure

The partition function of a pure lattice gauge theory is defined by

$$Z(\beta) = \int \prod_{x,\mu} dU_\mu(x) e^{-\beta S[U]}, \quad (58)$$

where the action is given by Eq. (52).

This is the analog of a partition function in statistical mechanics at an inverse temperature β given by

$$\beta = \frac{N}{g^2}. \quad (59)$$

This formula results from comparing Eq. (57) with the gauge-field part of the continuum action (25).

A subtle question is what is the measure $dU_\mu(x)$ in Eq. (58). To preserve the gauge invariance at finite lattice spacing, the integration is over the Haar measure which is an invariant group measure. The invariance of the

Haar measure under multiplication by an arbitrary group element from the left or from the right:

$$dU = d(\Omega U) = d(U \Omega'), \quad (60)$$

guarantees the gauge invariance of the partition function (58).

This invariance of the Haar measure is crucial for the Wilson formulation of lattice gauge theories.

An explicit expression for the Haar measure can be written for the $SU(2)$ gauge group, whose element is parametrized by a unit four-vector a_μ :

$$U = a_4 I + i \vec{a} \vec{\sigma} \quad a_\mu^2 = 1, \quad (61)$$

where $\vec{\sigma}$ are the Pauli matrices. The Haar measure for $SU(2)$ is

$$dU = \frac{1}{\pi^2} \prod_{\mu=1}^4 da_\mu \delta^{(1)}(a_\mu^2 - 1), \quad (62)$$

since $\det U = a_\mu^2$.

The partition function (58) characterizes vacuum effects in quantum theory. Physical quantities are given by the averages

$$\langle F[U] \rangle = Z^{-1}(\beta) \int \prod_{x,\mu} dU_\mu(x) e^{-\beta S[U]} F[U], \quad (63)$$

where $F[U]$ is a gauge-invariant functional of $U_\mu(x)$. These become the expectation values in the continuum theory as $a \rightarrow 0$ and $\beta = N/g^2$.

V. WILSON LOOPS ON A LATTICE

Lattice phase factors are associated with paths drawn on the lattice.

To write down the phase factor on the lattice via the link variables, let us specify the (lattice) contour C by its initial point x and by the directions (some may be negative) of the links forming the contour

$$C = \{x; \mu_1, \dots, \mu_n\}. \quad (64)$$

The lattice phase factor $U(C)$ is given by

$$U(C) = U_{\mu_n}(x + a\hat{\mu}_1 + \dots + a\hat{\mu}_{n-1}) \dots \times U_{\mu_2}(x + a\hat{\mu}_1) U_{\mu_1}(x). \quad (65)$$

For the links with a negative direction, it is again convenient to use Eq. (47).

A closed contour has $\hat{\mu}_1 + \dots + \hat{\mu}_n = 0$. The gauge invariant trace of the phase factor for a closed contour is called the Wilson loop.

The average of the Wilson loop is determined to be

$$\begin{aligned} W(C) &\equiv \left\langle \frac{1}{N} \text{tr } U(C) \right\rangle \\ &= Z^{-1}(\beta) \int \prod_{x,\mu} dU_\mu(x) e^{-\beta S[U]} \frac{1}{N} \text{tr } U(C). \end{aligned} \quad (66)$$

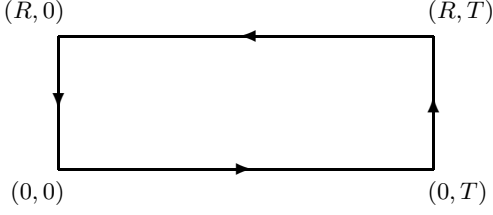


FIG. 5: Rectangular Wilson loop.

This average is often called the Wilson loop average.

A very important role is played by the Wilson loop averages for rectangular contours. Such a contour lying in the (x, t) -plane is depicted in Fig. 5. This rectangular Wilson loop is of the size $R \times T$.

The Wilson loop average is related for $T \gg R$ to the interaction energy of the static (i.e. infinitely heavy) quarks, separated by a distance R , by the formula

$$W(R \times T) \stackrel{T \gg R}{\propto} e^{-E_0(R)T}. \quad (67)$$

It can be proved in the axial gauge $\mathcal{A}_4 = 0$, where $U_4(x) = 1$ so that only vertical segments contribute to $U(R \times T)$. Denoting

$$\Psi_{ij}(t) \equiv \left[P e^{\int_0^R dz_1 A_1(z_1, \dots, t)} \right]_{ij}, \quad (68)$$

we have

$$W(R \times T) = \left\langle \frac{1}{N} \text{tr} \Psi(0) \Psi^\dagger(T) \right\rangle. \quad (69)$$

Inserting a sum over a complete set of intermediate states

$$\sum_n |n\rangle \langle n| = 1, \quad (70)$$

we obtain

$$\begin{aligned} W(R \times T) &= \sum_n \frac{1}{N} \langle \Psi_{ij}(0) | n \rangle \langle n | \Psi_{ji}^\dagger(T) \rangle \\ &= \sum_n \frac{1}{N} |\langle \Psi_{ij}(0) | n \rangle|^2 e^{-E_n T}, \end{aligned} \quad (71)$$

where E_n is the energy of the state $|n\rangle$. As $T \rightarrow \infty$, only the ground state with the lowest energy survives in the

sum over states and finally we find

$$W(R \times T) \xrightarrow{\text{large } T} e^{-E_0(R)T}. \quad (72)$$

Since nothing in the derivation relies on the lattice, it holds for a rectangular loop in the continuum theory as well.

VI. STRONG-COUPLING EXPANSION

Lattice path integrals can be calculated either by perturbation theory in g^2 or by an expansion in $\beta \propto 1/g^2$. This is called the strong-coupling expansion in analogy of the high-temperature expansion in statistical mechanics since β is the analog of inverse temperature.

To perform the strong-coupling expansion, we expand the exponential of the lattice action in β . Then the problem is to calculate the integrals over unitary group:

$$I_{j_1 \dots j_m, l_1 \dots l_n}^{i_1 \dots i_m, k_1 \dots k_n} = \int dU U_{j_1}^{i_1} \dots U_{j_m}^{i_m} U_{l_1}^{\dagger k_1} \dots U_{l_n}^{\dagger k_n}, \quad (73)$$

where the Haar measure is normalized

$$\int dU = 1. \quad (74)$$

The integral (73) is nonvanishing only if $n = m \pmod{N}$, i.e. if $n = m + kN$ with integer k .

For the simplest case of $m = n = 1$, the answer can easily be found by using the unitarity of U and the orthogonality relation

$$\int dU U_j^i U_l^{\dagger k} = \frac{1}{N} \delta_l^i \delta_j^k. \quad (75)$$

The simplest Wilson loop average is that for the loop which coincides with the boundary of a plaquette. It is called the plaquette average

$$W(\partial p) = \left\langle \frac{1}{N} \text{tr} U(\partial p) \right\rangle. \quad (76)$$

To calculate the plaquette average to order β , it is sufficient to retain only the terms $\mathcal{O}(\beta)$ in the expansion of the exponentials:

$$W(\partial p) = \frac{\int \prod_{x, \mu} dU_\mu(x) \left[1 + \beta \sum_{p'} \frac{1}{N} \text{Re tr} U(\partial p') \right] \frac{1}{N} \text{tr} U(\partial p)}{\int \prod_{x, \mu} dU_\mu(x) \left[1 + \beta \sum_{p'} \frac{1}{N} \text{Re tr} U(\partial p') \right]} + \mathcal{O}(\beta^2). \quad (77)$$

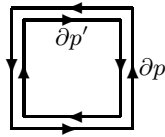


FIG. 6: Boundaries of plaquettes with opposite orientations.

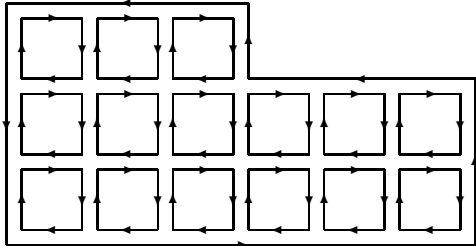


FIG. 7: Filling of a loop with plaquettes.

The group integration can then be performed by remembering that

$$\int dU_\mu(x) [U_\mu(x)]_j^i [U_\nu^\dagger(y)]_l^k = \frac{1}{N} \delta_{xy} \delta_{\mu\nu} \delta_l^i \delta_j^k \quad (78)$$

at different links.

Using this property of the group integral in Eq. (77), we immediately see that the denominator is equal to 1 (each link is encountered no more than once), while the only nonvanishing contribution in the numerator is from the plaquette p' , which coincides with p but has the opposite orientation as is depicted in Fig. 6. The boundaries of the plaquettes p and p' have opposite orientations ∂p and $\partial p'$, respectively.

The final answer for the plaquette average is

$$\left. \begin{aligned} W(\partial p) &= \frac{\beta}{2N^2} && \text{for } SU(N) \text{ with } N \geq 3, \\ W(\partial p) &= \frac{\beta}{4} && \text{for } SU(2). \end{aligned} \right\} \quad (79)$$

The result for $SU(2)$ differs by a factor of 1/2 because $\text{tr} U(\partial p)$ is real for $SU(2)$ so that the orientation of the plaquettes can be ignored.

According to Eq. (78), a nonvanishing result emerges only when plaquettes, arising from the expansion of the exponentials of Eq. (66) in β , completely cover a surface enclosed by the given loop C as is shown in Fig. 7. In this case each link is encountered twice (or never), once in the positive direction and once in the negative direction, so that all the group integrals are nonvanishing.

The leading order in β corresponds to filling a minimal surface:

$$W(C) = [W(\partial p)]^{A_{\min}(C)}, \quad (80)$$

where $W(\partial p)$ is given by Eq. (79) and $A_{\min}(C)$ is the area (in units of a^2) of the minimal surface. For a rectangle

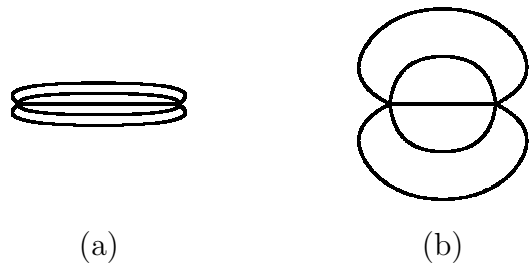


FIG. 8: Lines of force between static quarks.

the minimal surface is a piece of the plane:

$$W(R \times T) = [W(\partial p)]^{RT} \quad (81)$$

to the leading order in β .

Contribution of more complicated surfaces, do not lying in the plane of the rectangle, is $W(C) \sim \beta^{\text{area}}$ and is, therefore, suppressed since their areas are larger than A_{\min} .

VII. AREA LAW AND CONFINEMENT

The exponential dependence of the Wilson loop average on the area of the minimal surface (as in Eq. (80)) is called the area law. It is customarily assumed that if an area law holds for loops of large area in the pure $SU(3)$ gauge theory then quarks are confined. In other words, there are no physical $|in\rangle$ or $\langle out|$ quark states. This is the essence of Wilson's confinement criterion. The argument is that physical amplitudes (*e.g.*, the polarization operator) do not have quark singularities when the Wilson criterion is satisfied.

A. Linear potential

A justification for the Wilson criterion is based on the relationship (67) between the Wilson loop average and the potential energy of interaction between static quarks. When the area law

$$W(C) \xrightarrow{\text{large } C} e^{-KA_{\min}(C)} \quad (82)$$

holds for large loops, the potential energy is a linear function of the distance between the quarks:

$$E(R) = KR. \quad (83)$$

Lines of force between static quarks are depicted in Fig. 8 for (a) linear and (b) Coulomb interaction potentials. For the linear potential the lines of force are contracted into a tube, while they are distributed over the whole space for the Coulomb one.

The coefficient K is called the string tension because the gluon field between quarks contracts to a tube or string, whose energy is proportional to its length. The

value of K is the energy of the string per unit length. This string is stretched with the distance between quarks and prevents them from moving apart to macroscopic distances.

Equation (81) gives

$$K = \frac{1}{a^2} \ln \frac{2N^2}{\beta} = \frac{1}{a^2} \ln (2Ng^2) \quad (84)$$

for the string tension to the leading order of the strong-coupling expansion. The next orders of the strong-coupling expansion result in corrections in β to this formula. Confinement holds in the lattice gauge theory to any order of the strong-coupling expansion.

B. Asymptotic scaling

Equation (84) establishes the relationship between lattice spacing a and the coupling g^2 . Let K equals its experimental value

$$K = (400 \text{ MeV})^2 \approx 1 \text{ GeV/fm} \quad (85)$$

which results from the slope of the Regge trajectory $\alpha' = 1/2\pi K$. The slope $\alpha' = 1 \text{ GeV}^{-2}$ from the $\rho - A_2 - g$ trajectory.

The renormalizability prescribes that variations of a , which plays the role of a lattice cutoff, and of the bare charge g^2 should be made simultaneously in order that K does not change.

Given Eq. (84), this procedure calls for $a \rightarrow \infty$ as $g^2 \rightarrow \infty$. In other words, the lattice spacing is large in the strong-coupling limit, compared with 1 fm. Such a coarse lattice cannot describe the continuum limit and, in particular, the rotational symmetry.

In order to pass to the continuum, the lattice spacing a should be decreased. Equation (84) shows that a decreases with decreasing g^2 . However, this formula ceases to be applicable in the intermediate region of $g^2 \sim 1$ and, therefore, $a \sim 1 \text{ fm}$.

To further decrease a , we further decrease g^2 . While no analytic formulas are available at intermediate values of g^2 , the expected relation between a and g^2 for small g^2 is predicted by the known two-loop Gell-Mann–Low function of QCD.

For pure $SU(3)$ Yang-Mills, Eq. (84) is replaced at small g^2 by

$$K = \text{const} \cdot \frac{1}{a^2} \left(\frac{8\pi^2}{11g^2} \right)^{\frac{102}{121}} e^{-8\pi^2/11g^2}, \quad (86)$$

where the two-loop Gell-Mann–Low function is used.

The exponential dependence of K on $1/g^2$ is called asymptotic scaling. Asymptotic scaling sets in for some value of $1/g^2$. The dependence of the string tension on $1/g^2$ is shown in Fig. 9. The strong-coupling formula (84) holds for small $1/g^2$. The asymptotic-scaling formula (86) sets in for large $1/g^2$. Both formulas are not applicable in the intermediate region $1/g^2 \sim 1$.

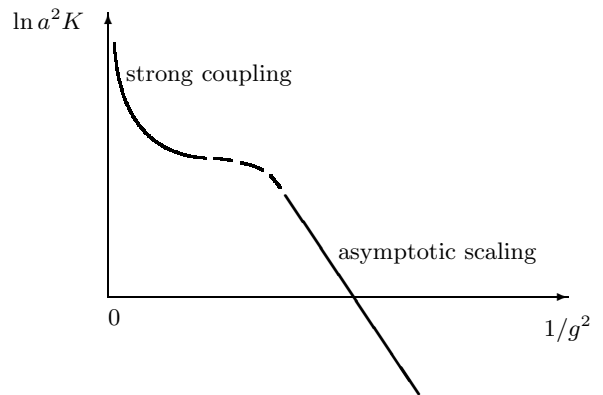


FIG. 9: String tension versus $1/g^2$

For such values of g^2 , where asymptotic scaling holds, the lattice gauge theory has a continuum limit.

The knowledge of the two asymptotic behaviors says nothing about the behavior of $a^2 K$ in the intermediate region of $g^2 \sim 1$. There can be either a smooth transition between these two regimes or a phase transition. Numerical methods were introduced to study this problem.

C. Relation to second-order phase transition

Continuum limits of a lattice system are reached at the points of second-order phase transitions when the correlation length becomes *infinite* in lattice units.

The correlation length is inversely proportional to Λ_{QCD} :

$$\xi \sim \Lambda_{\text{QCD}}^{-1} = a \exp \left[\int \frac{dg^2}{\mathcal{B}(g^2)} \right], \quad (87)$$

where $\mathcal{B}(g^2)$ is the Gell-Mann–Low function. The only chance for the RHS to diverge is to have a zero of $\mathcal{B}(g^2)$ at some fixed point $g^2 = g_*^2$. Therefore, the bare coupling should approach the fixed-point value g_*^2 to describe the continuum.

$\mathcal{B}(0) = 0$ for a non-Abelian gauge theory so that $g_*^2 = 0$ is a fixed-point value of the coupling constant. Therefore, the continuum limit is associated with $g^2 \rightarrow 0$.

Lecture III

$1/N$ Expansion

An effective coupling constant of QCD becomes large at large distances, so fluctuations of scales of different orders of magnitude are essential and there is no small parameter. 't Hooft proposed in 1974 [7] to use the number of colors N of the gauge group $SU(N)$ as such a parameter

and to perform an expansion in $1/N$. The motivation was the $1/N$ -expansion in statistical mechanics.

The $1/N$ -expansion of QCD rearranges perturbation theory in a way consistent with a string picture. The accuracy of large- N QCD is of the order of the ratios of meson widths to their masses (10–15%). While QCD is simplified in the large- N limit, it is not yet solved.

VIII. INDEX OR RIBBON GRAPHS

In order to describe the $1/N$ -expansion of QCD, it is convenient to use the matrix-field representation

$$[A_\mu(x)]^{ij} = \sum_a A_\mu^a(x) [t^a]^{ij}. \quad (88)$$

The matrix (88) is Hermitian and differs from (17) by g .

The propagator of the matrix field $A^{ij}(x)$ reads

$$\langle A_\mu^{ij}(x) A_\nu^{kl}(y) \rangle_{\text{Gauss}} = \left(\delta^{il} \delta^{kj} - \frac{1}{N} \delta^{ij} \delta^{kl} \right) D_{\mu\nu}(x-y), \quad (89)$$

where we have assumed, as usual, a gauge-fixing to define the gluon propagator in perturbation theory. For instance, one has¹

$$D_{\mu\nu}(x-y) = \frac{1}{4\pi^2} \frac{\delta_{\mu\nu}}{(x-y)^2} \quad (90)$$

in the Feynman gauge.

Equation (89) can be derived immediately from the standard formula

$$\langle A_\mu^a(x) A_\nu^b(y) \rangle_{\text{Gauss}} = \delta^{ab} D_{\mu\nu}(x-y) \quad (91)$$

multiplying by the generators of the $SU(N)$ gauge group according to the definition (88) and using the completeness condition

$$\sum_{a=1}^{N^2-1} (t^a)^{ij} (t^a)^{kl} = \left(\delta^{il} \delta^{kj} - \frac{1}{N} \delta^{ij} \delta^{kl} \right) \boxed{\text{for } SU(N)}. \quad (92)$$

Alternatively, Eq. (89) can be derived directly from a path integral over the matrix fields.

We concentrate only on the structure of diagrams in the index space, i.e. the space of the indices associated with the $SU(N)$ group. We shall not consider, in most cases, space-time structures of diagrams which are prescribed by Feynman's rules.

Omitting at large N the second term in parentheses on the RHS of Eq. (89), we depict the propagator by the *double line*

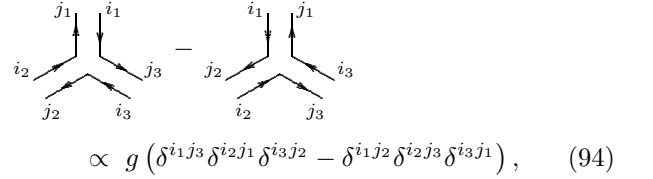
$$\langle A_\mu^{ij}(x) A_\nu^{kl}(y) \rangle_{\text{Gauss}} \propto \delta^{il} \delta^{kj} = \begin{array}{c} i \longrightarrow l \\ j \longleftarrow k \end{array}. \quad (93)$$

Each line, often termed the index line, represents the Kronecker delta-symbol and has an orientation which is indicated by arrows. This notation is obviously consistent with the space-time structure of the propagator that describes a propagation from x to y .

Arrows are a result of the fact that the matrix A_μ^{ij} is Hermitian and its off-diagonal components are complex conjugate.

Double lines appear generically in all models describing matrix fields in contrast to vector (in internal symmetry space) fields, whose propagators are depicted by single lines.

The three-gluon vertex is depicted in the double-line notation as

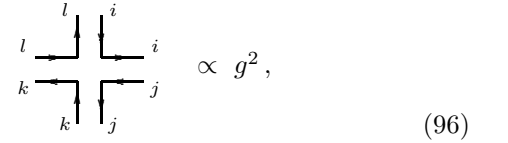


where the subscripts 1, 2 or 3 refer to each of the three gluons. The relative minus sign arises from the commutator in the cubic-in- A term in the action (25). The color part is antisymmetric under an interchange of gluons. The (momentum space) space-time part

$$\begin{aligned} \gamma_{\mu_1 \mu_2 \mu_3}(p_1, p_2, p_3) &= \delta_{\mu_1 \mu_2} (p_1 - p_2)_{\mu_3} \\ &+ \delta_{\mu_2 \mu_3} (p_2 - p_3)_{\mu_1} + \delta_{\mu_1 \mu_3} (p_3 - p_1)_{\mu_2} \end{aligned} \quad (95)$$

is also antisymmetric. We consider all three gluons as incoming so their momenta obey $p_1 + p_2 + p_3 = 0$. The full vertex is symmetric as is prescribed by Bose statistics.

The four-gluon vertex involves six terms – each of them is depicted by a cross – which differ by interchanging of the color indices. We depict the color structure of the four-gluon vertex for simplicity in the case when $i_1 = j_2 = i$, $i_2 = j_3 = j$, $i_3 = j_4 = k$, $i_4 = j_1 = l$, but i, j, k, l take on different values. Then only the following term is left:



where there are no delta-symbols since the color structure is fixed. We pick up only one color structure by equating indices pairwise.

Diagrams of perturbation theory can now be completely rewritten in the double-line notation. The simplest one describing the one-loop correction to the gluon propagator is depicted in Fig. 10. The sum over the N indices is associated with the closed index line. The contribution of this diagram is $\sim g^2 N \sim 1$.

In order for the large- N limit to be nontrivial, the bare coupling constant g^2 should satisfy

$$g^2 \sim \frac{1}{N}. \quad (97)$$

¹ Here and in Eq. (95) $\delta_{\mu\nu}$ is due to Euclidean metric and is to be substituted by $-g_{\mu\nu}$ in Minkowski space.

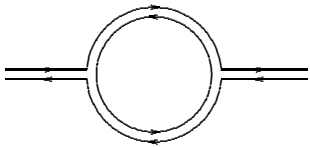


FIG. 10: Double-line representation of a one-loop diagram for gluon propagator.

This dependence on N is also prescribed by the asymptotic-freedom formula

$$g^2 = \frac{12\pi^2}{11N \ln(\Lambda/\Lambda_{\text{QCD}})} \quad (98)$$

of the pure $SU(N)$ gauge theory.

Thus, the contribution of the diagram in Fig. 10 is of order $\sim g^2 N \sim 1$ in the large- N limit.

The double lines can be viewed as bounding a piece of a plane. These lines represent a two-dimensional object. In mathematics these double-line graphs are often called ribbon graphs or fatgraphs. They are connected with Riemann surfaces.

Remark on the $U(N)$ gauge group

The double-line representation of the diagrams holds, strictly speaking, only for the $U(N)$ gauge group, whose generators

$$T^A = \left(t^a, I/\sqrt{N} \right), \quad \text{tr} T^A T^B = \delta^{AB} \quad \boxed{A = 1, \dots, N^2}. \quad (99)$$

obey the completeness condition

$$\sum_{A=1}^{N^2} (T^A)^{ij} (T^A)^{kl} = \delta^{il} \delta^{kj} \quad \boxed{\text{for } U(N)}. \quad (100)$$

Elements of both $SU(N)$ and $U(N)$ can be represented in the form

$$U = e^{iB}, \quad (101)$$

where B is a general Hermitian matrix for $U(N)$ and a traceless Hermitian matrix for $SU(N)$.

The large- N limit of both the $U(N)$ and $SU(N)$ groups is the same.

IX. PLANAR AND NONPLANAR GRAPHS

The double-line representation of perturbation-theory diagrams is very convenient to estimate their orders in $1/N$. Each three- or four-gluon vertex contributes a factor of g or g^2 , respectively. Each closed index line contributes a factor of N , while $g^2 \sim 1/N$.

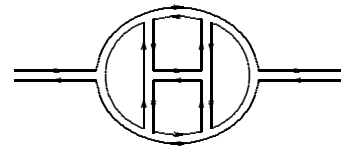


FIG. 11: Double-line representation of a four-loop diagram.

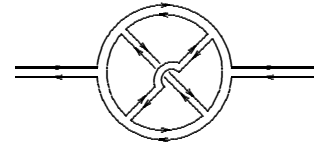


FIG. 12: Double-line representation of a nonplanar diagram.

A. 't Hooft topological expansion

Let us consider a typical diagram for the gluon propagator depicted in Fig. 11. The sum over the N indices is associated with each of the four closed index lines, whose number is equal to the number of loops. The contribution of this diagram is $\sim g^8 N^4 \sim 1$.

Diagrams of this type, which can be drawn on a sheet of paper without crossing any lines, are called planar diagrams. For such diagrams, the addition of a loop inevitably results in the addition of two three-gluon (or one four-gluon) vertices. A planar diagram with n_2 loops has n_2 closed index lines. It is of order

$$n_2\text{-loop planar diagram} \sim (g^2 N)^{n_2} \sim 1, \quad (102)$$

so that all planar diagrams survive in the large- N limit.

Let us now consider a nonplanar diagram of the type depicted in Fig. 12. The diagram has six three-gluon vertices but only one closed index line (although it has three loops!). The order of this diagram is $\sim g^6 N \sim 1/N^2$.

This nonplanar diagram can be drawn without line-crossing on a surface with one handle (or hole) which in mathematics is called a torus or a surface of genus one. A plane is then equivalent to a sphere and has genus zero. A general Riemann surface with h holes has genus h .

The above evaluations of the order of the diagrams can be described by the single formula

$$\text{genus-}h \text{ diagram} \sim \left(\frac{1}{N^2} \right)^{\text{genus}}. \quad (103)$$

The expansion in $1/N$ rearranges perturbation-theory diagrams according to their topology as demonstrated in 1974 by 't Hooft [7]. It is referred to as the topological expansion or the genus expansion.

Only planar diagrams associated with genus zero survive in the large- N limit. The problem of summing the planar graphs is complicated but simpler than that of summing all the graphs, since the number of planar

graphs with n_0 vertices grows geometrically at large n_0 :

$$\#_p(n_0) \equiv \text{no of planar graphs} \sim \text{const}^{n_0}, \quad (104)$$

as shown by Tuttle [8] and Koplik, Neveu, Nussinov [9], while the total number of graphs grows factorially with n_0 . There is no dependence in Eq. (104) on the number of external lines of a planar graph which is assumed to be much less than n_0 .

There is a big difference between the planar diagrams and the ladder diagrams which describe e^+e^- elastic scattering in QED. For the ladder with n rungs, there are $n!$ ladder diagrams, but only one of them is planar. This shows why the number of planar graphs is much smaller than the total number of graphs, most of which are non-

planar.

B. Topological expansion (continued)

Equation (103) holds, strictly speaking, only for the gluon propagator, while the contribution of all planar diagrams to a connected n -point Green function is $\sim g^{n-2}$, which is its natural order in $1/N$. The three-gluon Green function is $\sim g$, the four-gluon one is $\sim g^2$ and so on. The contributions of all planar diagrams are of the same order ~ 1 in the large- N limit, independently of the number of external lines, for the Wilson loop average

$$\left\langle \frac{1}{N} \text{tr} P e^{ig \oint_{\Gamma} dx^{\mu} A_{\mu}(x)} \right\rangle = \sum_{n=0}^{\infty} g^n \oint_{\Gamma} dx_1^{\mu_1} \int_{x_1}^{x_2} dx_2^{\mu_2} \dots \int_{x_1}^{x_{n-1}} dx_n^{\mu_n} G_{\mu_1 \dots \mu_n}^{(n)}(x_1, \dots, x_n) \quad (105)$$

with

$$G_{\mu_1 \dots \mu_n}^{(n)}(x_1, \dots, x_n) \equiv \frac{g^n}{N} \langle \text{tr} [A_{\mu_1}(x_1) \dots A_{\mu_n}(x_n)] \rangle. \quad (106)$$

The factor of $1/N$, which normalizes the trace, provides the natural normalization. The ordering along a closed path implies cyclic-ordering in the index space as depicted in Fig. 13, where we omit the arrows for simplicity. This diagram has $n_0 = 10$ vertices, $n_1 = 12$ gluon propagators, $n_2 = 4$ closed index lines, and $B = 1$ boundary. The color indices of the external lines are contracted by the Kronecker delta-symbols (represented by the single lines) in a cyclic order. The extra factor of $1/N$ arises from the normalization. The order in $1/N$ of the diagram in Fig. 13 is $\sim 1/N^2$ in accord with Eq. (103).

Analogously, the color indices in Eq. (106) are contracted in the cyclic order. The delta-symbols, which contract the color indices, are depicted by the single lines. They can be viewed as a boundary of the diagram. The actual size of the boundary is not essential – it can be

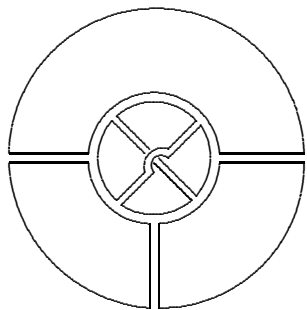


FIG. 13: Generic double-line index diagram.

shrunk to a point. Then a bounded piece of a plane will be topologically equivalent to a sphere with a puncture. We draw planar diagrams in a plane with an extended boundary (boundaries) rather than in a sphere with a puncture (punctures). The closed boundary is associated with the trace over the color indices of the multi-point Green function

The boundary represents the Wilson loop = a trajectory of a heavy quark in the fundamental representation.

C. Topological expansion and quark loops

It is easy to incorporate quarks in the topological expansion. A quark field belongs to the fundamental representation of the gauge group $SU(N)$ and its propagator is represented by a single line

$$\langle \psi_i \bar{\psi}_j \rangle \propto \delta_{ij} = i \longrightarrow j. \quad (107)$$

The arrow indicates, as usual, the direction of propagation of a (complex) field ψ . These arrows are often omitted for simplicity.

The diagram for the gluon propagator which involves one quark loop is depicted in Fig. 14a. It involves one quark loop and has no closed index lines so that its order is $\sim g^2 \sim 1/N$. The diagram in Fig. 14b is $\sim g^6 N^2 \sim 1/N$ analogously.

It is evident from this consideration that quark loops are not accompanied by closed index lines. One should add a closed index line for each quark loop in order for a given diagram with L quark loops to have the same double-line representation as for pure gluon diagrams. Therefore, given Eq. (103), diagrams with L quark loops

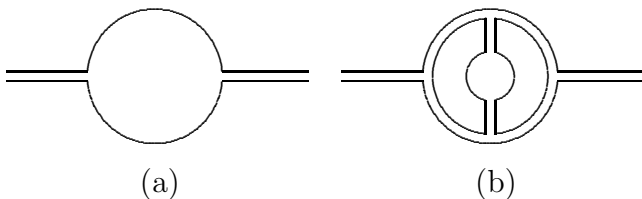


FIG. 14: Diagrams for gluon propagator which involve quark loop.

are suppressed at large N by

$$L \text{ quark loops} \sim \left(\frac{1}{N}\right)^{L+2 \cdot \text{genus}}. \quad (108)$$

The single-line representation of the quark loops is similar to that of the Wilson loop. Such a diagram emerges in gluon corrections to the vacuum expectation value of the quark operator

$$O = \frac{1}{N} \bar{\psi} \psi, \quad (109)$$

where the factor of $1/N$ is introduced to make it $\mathcal{O}(1)$ in the large- N limit. Therefore, the external boundary can be viewed as a single line associated with valence quarks.

D. The proof of topological expansion

To prove Eqs. (103) and its quark counterpart (108), let us consider a generic diagram in the index space which has $n_0^{(3)}$ three-point vertices (either three-gluon or quark-gluon ones), $n_0^{(4)}$ four-gluon vertices, n_1 propagators (either gluon or quark ones), n_2 closed index lines, L virtual quark loops and B external boundaries. Its order in $1/N$ is

$$\frac{1}{N^B} g^{n_0^{(3)}+2n_0^{(4)}} N^{n_2} \sim N^{n_2-n_0^{(3)}/2-n_0^{(4)}-B} \quad (110)$$

as has already been explained. The extra factor of $1/N^B$ arises from the extra normalization factor of $1/N$ in operators associated with external boundaries.

The number of propagators and vertices are related by

$$2n_1 = 3n_0^{(3)} + 4n_0^{(4)}, \quad (111)$$

since three- and four-point vertices emit three or four propagators, respectively, and each propagator connects two vertices. We then rewrite the RHS of (110) as

$$N^{n_2-n_0^{(3)}/2-n_0^{(4)}-B} = N^{n_2-n_1+n_0-B}, \quad (112)$$

where $n_0 = n_0^{(3)} + n_0^{(4)}$ is the total number of vertices.

The exponent on the RHS of Eq. (112) can be expressed via the Euler characteristic χ of a given graph of genus h . An appropriate Riemann surface, which is

associated with a given graph, is open and has $B + L$ boundaries. This surface can be closed by attaching a cap to each boundary. The single lines then become double lines together with the lines of the boundary of each cap. We have already considered this procedure when deducing Eq. (108) from Eq. (103).

The number of faces for a closed Riemann surface constructed in such a manner is $n_2 + L + B$, while the number of edges and vertices are n_1 and n_0 , respectively. Euler's theorem states that

$$\chi \equiv 2 - 2h = n_2 + L + B - n_1 + n_0. \quad (113)$$

Therefore the RHS of Eq. (112) can be rewritten as

$$N^{n_2-n_1+n_0-B} = N^{2-2h-L-2B}. \quad (114)$$

We have thus proven that the order in $1/N$ of a generic graph does not depend on its order in the coupling constant and is completely expressed via the genus h and the number of virtual quark loops L and external boundaries B by

$$\text{generic graph} \sim \left(\frac{1}{N}\right)^{2h+L+2(B-1)}. \quad (115)$$

For $B = 1$, we recover Eqs. (103) and (108).

E. 't Hooft versus Veneziano limits

In QCD there are several species or flavors of quarks (u -, d -, s - and so on). We denote the number of flavors by N_f and associate a Greek letter α or β with a flavor index of the quark field.

The quark propagator then has the Kronecker delta-symbol with respect to the flavor indices in addition to Eq. (107):

$$\langle \psi_i^\alpha \bar{\psi}_j^\beta \rangle \propto \delta^{\alpha\beta} \delta_{ij}. \quad (116)$$

Their contraction results in

$$\sum_{\alpha=1}^{N_f} \delta_{\alpha\alpha} = N_f. \quad (117)$$

Therefore, an extra factor of N_f corresponds to each closed quark loop for the N_f flavors.

The limit when N_f is fixed as $N \rightarrow \infty$ is called the 't Hooft limit. Only valence quarks are then left (the quenched approximation). In order for a meson to decay into other mesons built out of quarks, a quark-antiquark pair must be produced out of the vacuum. Consequently, the ratios of meson widths to their masses are

$$\frac{\Gamma_{\text{total}}}{M} \sim \frac{N_f}{N} \quad (118)$$

in the 't Hooft limit. The ratio on the LHS of Eq. (118) is 10–15% experimentally for the ρ -meson. The hope of

solving QCD in the 't Hooft limit is the hope to describe QCD with this accuracy.

An alternative large- N limit of QCD, when $N_f \sim N$ as $N \rightarrow \infty$, was proposed by Veneziano in 1976 [10]. A general diagram with L quark loops will contribute

$$L \text{ quark loops} \sim \left(\frac{N_f}{N}\right)^L \left(\frac{1}{N^2}\right)^{\text{genus}}, \quad (119)$$

since each quark loop results in N_f .

The quark loops are not suppressed at large N in the Veneziano limit

$$N_f \sim N \rightarrow \infty \quad (120)$$

if the diagram is planar.

It is the Veneziano limit that is related to the hadronic topological expansion in the dual-resonance models. In the Veneziano limit hadrons can have finite widths according to Eq. (118).

X. LARGE- N FACTORIZATION

The vacuum expectation values of several colorless or white operators, which are singlets with respect to the gauge group, factorize in the large- N limit of QCD (or other matrix models) as was first noticed by A. A. Migdal and independently E. Witten in late 1970's.

The simplest gauge-invariant operators in a pure $SU(N)$ gauge theory are the closed Wilson loops

$$\Phi(C) = \frac{1}{N} \text{tr} P e^{ig \oint_C dz^\mu A_\mu(z)}. \quad (121)$$

They obey the factorization property

$$\langle \Phi(C_1) \cdots \Phi(C_n) \rangle = \langle \Phi(C_1) \rangle \cdots \langle \Phi(C_n) \rangle + \mathcal{O}(N^{-2}). \quad (122)$$

The factorization implies a semiclassical nature of the large- N limit of QCD (a saddle point in the path integral for certain variables).

The factorization property also holds for gauge-invariant operators constructed from quarks as in Eq. (109). For the case of several flavors N_f , we normalize these quark operators by

$$O_\Gamma = \frac{1}{N_f N} \bar{\psi} \Gamma \psi. \quad (123)$$

Here Γ denotes one of the combination of the γ -matrices:

$$\Gamma = I, \gamma_5, \gamma_\mu, \gamma_\mu \gamma_5, \Sigma_{\mu\nu} = \frac{1}{2i} [\gamma_\mu, \gamma_\nu], \dots \quad (124)$$

The factorization of the gauge-invariant quark operators holds both in the 't Hooft and Veneziano limits:

$$\langle O_{\Gamma_1} \cdots O_{\Gamma_n} \rangle = \langle O_{\Gamma_1} \rangle \cdots \langle O_{\Gamma_n} \rangle + \mathcal{O}(1/(N_f N)). \quad (125)$$

The nonfactorized part, which is associated with connected diagrams, is $\sim 1/N$ in the 't Hooft limit. This leads, in particular, to the coupling constant of meson-meson interaction of order $1/N$. The Veneziano limit is analogous to pure Yang-Mills.

The factorization can be seen (at all orders of perturbation theory) from Eq. (115) for the contribution of a generic connected graph of genus h with B external boundaries which are precisely associated with the Wilson loops (or the quark operators O_Γ). The diagrams with gluon lines emitted and absorbed by the same operator are products of diagrams having only one boundary. Their contribution is of order one. The diagrams with gluon lines emitted and absorbed by two different operators have two boundaries. This proves the factorization property (125) at all orders of perturbation theory.

The large- N factorization can also be verified beyond perturbation theory at all orders of the strong-coupling expansion in the $SU(N)$ lattice gauge theory. A non-perturbative proof of the factorization was given using quantum equations of motion (the loop equations) [11].

XI. CONCLUSION

We have considered in these lecture notes the basic features of the methods for nonperturbative studies of gauge theories, which were developed in the second half of 1970's – early 1980's. Their contemporary applications in high-energy physics are extremely broad: from the scattering of particles at very high energies to the attempts of constructing a unified theory of all interactions, including gravity. Some of these issues are considered in other lectures at this School.

[1] Y. Makeenko, *Methods of contemporary gauge theory* (Cambridge Univ. Press, 2002).
 [2] Y. Aharonov and D. Bohm, Phys. Rev. **115**, 485 (1959).
 [3] C.N. Yang and R.L. Mills, Phys. Rev. **96**, 191 (1954).
 [4] H. Weyl, Ann. der Phys. **59** v. 10, 101 (1919).
 [5] F. London, Z. Phys. **42**, 375 (1927).
 [6] K. G. Wilson, Phys. Rev. D **10**, 2445 (1974).
 [7] G. 't Hooft, Nucl. Phys. B **72**, 461 (1974).

[8] W.T. Tuttle, Can. J. Math. **14**, 21 (1962).
 [9] J. Koplik J., A. Neveu, and S. Nussinov, Nucl. Phys. B **123**, 109 (1977).
 [10] G. Veneziano, Nucl. Phys. B **117**, 519 (1976).
 [11] Y. M. Makeenko and A. A. Migdal, Phys. Lett. B **88**, 135 (1979).